CHEMISTRY
A EUROPEAN JOURNAL

DOI: 10.1002/chem.200801658

“Roll-over” Cyclometalation of 2,2′-Bipyridine Platinum(II) Complexes in the Gas Phase: A Combined Experimental and Computational Study

Burkhard Butschke,[a] Maria Schlangen,[a] Detlef Schröder,[b] and Helmut Schwarz*[a]

Dedicated to Professor Joachim Sauer on the occasion of his 60th birthday

Abstract: In a combined experimental/computational investigation, the gas-phase behavior of cationic $[Pt(bipy)(CH_3)((CH_3)_2S)]^+$ (**1**) (bipy = 2,2′-bipyridine) has been explored. Losses of CH_4 and $(CH_3)_2S$ from **1** result in the formation of a cyclometalated 2,2′-bipyrid-3-yl species $[Pt(bipy-H)]^+$ (**2**). As to the mechanisms of ligand evaporation, detailed labeling experiments complemented by DFT-based computations reveal that the reaction follows the mechanistically intriguing “roll-over” cyclometalation path in the course of which a hydrogen atom from the C(3)-position is combined with the Pt-bound methyl group to produce CH_4. Activation of a C−H-bond of the $(CH_3)_2S$ ligand occurs as well, but is less favored (35 % versus 65 %) as compared to the C(3)−H bond activation of bipy. In addition, the thermal ion/molecule reactions of $[Pt(bipy-H)]^+$ with $(CH_3)_2S$ have been examined, and for the major pathway, that is, the dehydrogenative coupling of the two methyl groups to form C_2H_4, a mechanism is suggested that is compatible with the experimental and computational findings. A hallmark of the gas-phase chemistry of $[Pt(bipy-H)]^+$ with the incoming $(CH_3)_2S$ ligand is the exchange of *one* (and only one) hydrogen atom of the bipy fragment with the C−H bonds of dimethylsulfide in a reversible “roll-over” cyclometalation reaction. The Pt^{II}-mediated conversion of $(CH_3)_2S$ to C_2H_4 may serve as a model to obtain mechanistic insight in the dehydrosulfurization of sulfur-containing hydrocarbons.

Keywords: bipyridine • bond activation • cyclometalation • dehydrosulfurization • platinum

Introduction

2,2′-Bipyridine (bipy) and related heterocyclic systems represent versatile ligands in the coordination chemistry of transition metals. Their complexes have received widespread interest, for example in the assembly of supramolecular networks,[1] to serve as molecular devices of photochemical relevance,[2] to act as pre-catalysts in polymerization processes,[3] to provide useful intermediates in synthesis,[4] or to afford insight in intrinsic reactivity features by probing their gas-phase properties.[5]

With regard to the timely topic of metal-mediated bond activation, the mechanistically intriguing “roll-over” cyclometalation of 2,2′-bipyridines, which entails a sequence of decomplexation, rotation around the central C(2)−C(2′) bond, and cleavage of the C(3)−H bond of a pyridine ring (Scheme 1), has received quite some attention.[6] While the structures of the resulting, still rather rare C−Pt cyclometalated 2,2′-bipyridines are now confirmed after a long and controversial debate, mechanistic details of the reaction are far from being settled conclusively.[6]

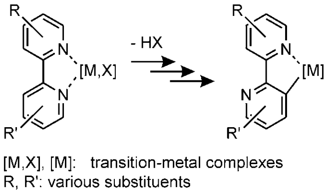

Scheme 1. “Roll-over” cyclometalation of 2,2′-bipyridines.

---

[a] B. Butschke, M. Schlangen, Prof. Dr. H. Schwarz
Institut für Chemie, Technische Universität Berlin
Straße des 17. Juni 135, 10623 Berlin (Germany)
Fax: (+49) 30-314-21102
E-mail: Helmut.Schwarz@mail.chem.tu-berlin.de

[b] Dr. D. Schröder
Institute of Organic Chemistry and Biochemistry
Flemingovo nám. 2, 16610 Prague (Czech Republic)

© 2008 Wiley-VCH Verlag GmbH & Co. KGaA, Weinheim

Here, we report gas-phase experiments of Pt^{II} complexes of 2,2′-bipyridine, generated by electrospray ionization (ESI)[7] and probed by mass-spectrometric methods. These experiments, complemented by labeling studies and density-functional calculations, provide for the first time evidence for the operation of the "roll-over" cyclometalation of an unsubstituted 2,2′-bipyridine by a "bare" cationic Pt^{II} core in the gas phase (Scheme 2).[8] In addition, mechanistic variants operative in the course of the ligand evaporation from $[Pt(bipy)(CH_3)((CH_3)_2S)]^+$ (**1**) will be discussed as well as unique interligand hydrogen-exchange processes that prevail in the dissociation of **1** and in the ion/molecule reactions (IMR) of the resulting product $[Pt(bipy-H)]^+$ ion (**2**) with neutral $(CH_3)_2S$.

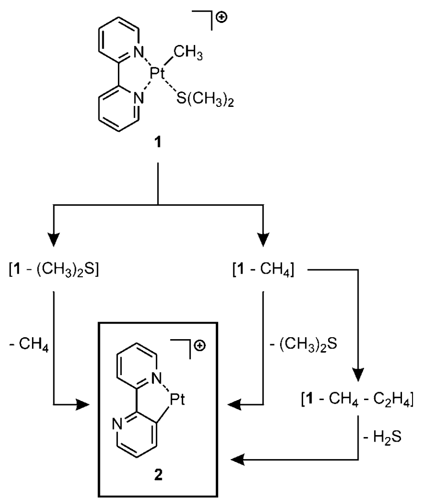

Scheme 2. Gas-phase generation of C-Pt cyclometalated 2,2′-bipyridine **2**. The path $\mathbf{1} \rightarrow [\mathbf{1}-(CH_3)_2S] \rightarrow \mathbf{2}$ is a high-energy process (see below) and does not compete at lower energies with the alternative sequence $\mathbf{1} \rightarrow [\mathbf{1}-CH_4] \rightarrow \mathbf{2}$.

Experimental and Computational Details

The present experiments were performed with a VG BIO-Q mass spectrometer of QHQ configuration (Q: quadrupole, H: hexapole) equipped with an ESI source as described in detail previously.[9] In brief, millimolar solutions of dimeric $[Pt(CH_3)_2(\mu\text{-}(CH_3)_2S)]_2$ (prepared according to reference[10]) and the desired ligand bipy (or analogous heterocycles) in pure methanol were introduced through a fused-silica capillary to the ESI source via a syringe pump (ca. 3 $\mu L\,min^{-1}$). All heterocyclic ligands employed were either purchased or synthesized according to literature-reported standard procedures. For the generation of complexes with $(CD_3)_2S$ as a ligand instead of $(CH_3)_2S$, an excess of $(CD_3)_2S$ was added to the solution. Nitrogen was used as a nebulizing and drying gas at a source temperature of 80 °C. Maximal yields of the desired $[Pt(bipy)(CH_3)((CH_3)_2S)]^+$ complex **1** and related platinum complexes were achieved by adjusting the cone voltage (U_c) between 20 and 60 V, which determines the degree of collisional activation of the incident ions in the transfer from the ESI source to the mass spectrometer.[11] The identity of the ions was confirmed by comparison with the expected isotope patterns,[12] collision-induced dissociation (CID) experiments, and extensive labeling studies. The isotope pattern also assisted in the choice of the adequate precursor ion in order to avoid coincidental mass overlaps of isobaric species in the mass-selected ion beam.[13] For CID experiments, the ions of interest were mass-selected using Q1, interacted with Xe as a collision gas (typically $p = 10^{-4}$ mbar) at variable collision energies of $E_{lab} = 0\text{–}20$ eV, while scanning Q2 to monitor the ionic products. Parent-ion scans, in which the first analyzer scans a regular mass spectrum while the second mass analyzer is fixed to the m/z value of the desired product ion, were used to identify all ions ("parents") which give rise to a particular product ion. The ion/molecule reactions of $[Pt(bipy-H)]^+$ (**2**) and related complexes with $(CH_3)_2S$ and its isotopologues were probed at a collision energy (E_{lab}) set to nominally 0 eV, which in conjunction with the ca. 0.4 eV kinetic energy width of the parent ion at peak half height[9a] allows the investigation of quasi-thermal reactions, as demonstrated previously.[14] In order to also recognize secondary reactions, the pressure of the neutral substrate was deliberately increased to multiple-collision conditions.[15] In the case of ion **2**, the ESI source was operated at a cone voltage of $U_c = 60$ V. Harsher conditions lead to further fragmentation and undesired overlap of isobaric signals, whereas lower cone voltages decrease the yield of the desired product ion **2**.

In the computational studies, which primarily aim at a qualitative description of the unimolecular reactions of **1** and the ion/molecule reactions of **2** with $(CH_3)_2S$, the geometries of all species were optimized at the B3LYP level of theory[16] as implemented in the Gaussian03 program package[17] using basis sets of approximately triple-ξ quality. For H, C, N, and S atoms these were the triple-ξ plus polarization basis sets (TZVP) of Ahlrichs and co-workers.[18] For platinum, the Stuttgart–Dresden scalar relativistic pseudopotential (ECP60MDF replacing 60 core electrons) was employed in conjunction with the corresponding (8s,7p,6d)/[6s,5p,3d] basis set describing the 6s5d valence shell of Pt.[19] The nature of the stationary structures as minima or saddle points was elucidated by frequency analysis, and intrinsic reaction coordinate (IRC) calculations were performed to link the transition structures with the respective intermediates.[20] Energies (given in $kJ\,mol^{-1}$) are corrected for (unscaled) zero-point vibrational energy contributions. The discussion of the computational findings will be confined to the singlet states of the various platinum cations, because exploratory calculations show that the triplet states are generally much higher in energy for all species investigated.

Results and Discussion

Under soft ionization conditions (i.e., U_c up to about 30 V), the ESI ion-source mass spectra of a methanolic solution of $[Pt(CH_3)_2(\mu\text{-}(CH_3)_2S)]_2$ and bipy (Figure 1) are dominated by a signal which we attribute to the formation of the cationic complex $[Pt(bipy)(CH_3)((CH_3)_2S)]^+$ (**1**). As expected, the extent of fragmentation of **1** increases with increasing U_c; the latter controls the amount of energizing collisions occurring in the source region.[9,11,21] When increasing the cone voltage starting from $U_c = 30$ V, one observes first the elimination of CH_4, then of $(CH_3)_2S$ and, at yet higher energies, a combination of the two neutral fragments resulting in the formation of $[Pt(bipy-H)]^+$ (**2**). In addition, some of the primary fragment ions undergo consecutive reactions, for example, the combined losses of CH_4 and C_2H_4 formally yielding $[\mathbf{1}-CH_4-C_2H_4]$.[22] As also shown in Figure 1, several ions form adducts with N_2 used as the drying gas in ESI and the amount of the N_2 complexes heavily depends on the experimental conditions chosen. Assignment of these ions as genuine N_2 complexes has been confirmed by variation of the ESI solvent, that is, CD_3OD and CH_3CN, and is also consistent with the data obtained in the labeling experiments.

The generation of the fragment ions is further elucidated by a series of CID spectra of mass-selected $[Pt(bipy)(CH_3)$-

© 2008 Wiley-VCH Verlag GmbH & Co. KGaA, Weinheim

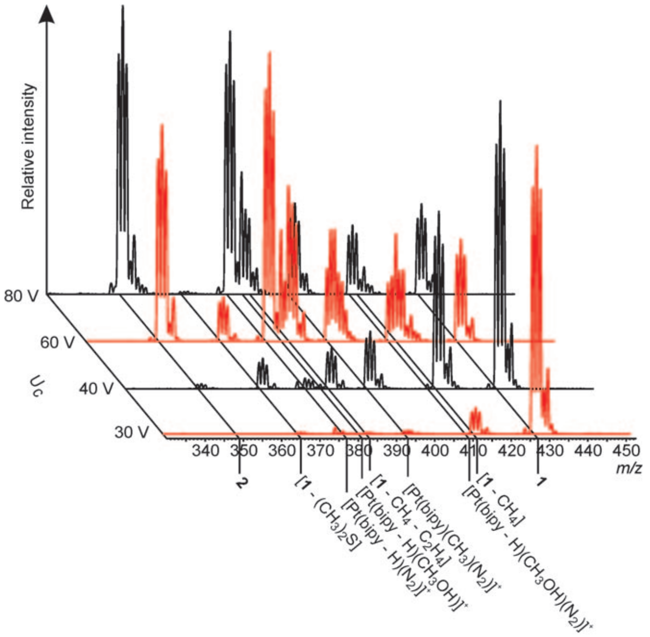

Figure 1. ESI-source mass spectra of a dilute methanolic solution of $[Pt(CH_3)_2(\mu\text{-}(CH_3)_2S)]_2$ and 2,2′-bipyridine at different cone voltages.

$((CH_3)_2S)]^+$ (**1**) which imply the sequence of dissociation reactions shown in Scheme 2. At low collision energies, the losses of methane and dimethylsulfide are observed as the first fragments with apparent thresholds of $AE(-CH_4) = (0.9 \pm 0.2)$ eV and $AE(-(CH_3)_2S) = (1.2 \pm 0.2)$ eV (Figure 2), where these values should only be considered as a rough orientation for the energy demands of the fragmentations.[23] Note further, that the threshold behavior of **1** is of composite nature and that there is another component, most likely a direct fragmentation pathway becoming predominant at a collision energy of about 3 eV. At a collision energy of about 2 eV, the combined loss of $CH_4/(CH_3)_2S$ starts to appear and the branching of these three channels (see inset in Figure 2) implies that this is mostly due to loss of CH_4 followed by that of $(CH_3)_2S$ because the [**1**−CH_4] fragment serves as a feed for the $[Pt(bipy-H)]^+$ fragment (**2**), whereas the fraction of [**1**−$(CH_3)_2S$] remains relatively constant. A parent-ion scan for **2** performed at $U_c = 30$ V further confirms the reaction sequence depicted in Scheme 2; we note in passing that also the N_2 clustered species $[Pt(bipy-H)(N_2)]^+$ and $[Pt(bipy)(CH_3)(N_2)]^+$ serve as "parents" for **2**. At elevated collision energies, also the expulsion of neutral Pt-species concomitant with formation of the protonated ligand LH^+ is observed; according to the labeling data, the additional proton stems from the dimethylsulfide ligand. According to the CID results, the formation of LH^+ occurs as a consecutive fragmentation of the primary fragments at elevated collision energies, e.g. [**1**−Me_2S]→$(bipy+H)^+ + PtCH_2$. Therefore, and because this reaction only occurs at higher energies and leads to the degradation of the platinum cations, this pathway is not discussed in further detail.

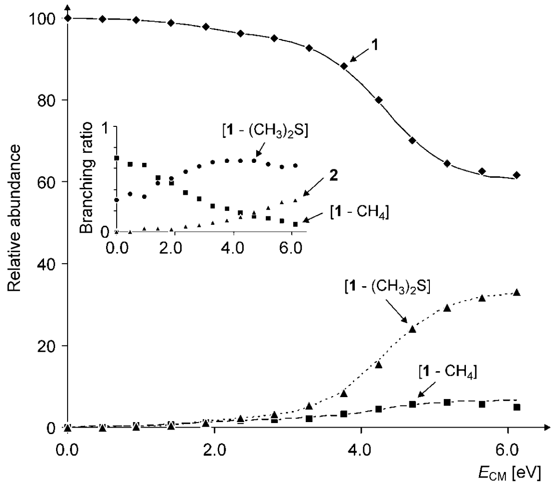

Figure 2. Energy dependence of the parent ion (◆) and the primary cationic fragments [**1**−$(CH_3)_2S$] (▲) and [**1**−CH_4] (■) in the CID spectra of mass-selected $[Pt(bipy)(CH_3)((CH_3)_2S)]^+$ (**1**) at various collision energies. Note that secondary fragments are summed into the ion abundances for the primary channels. The inset shows the branching ratio of the competing losses of CH_4 and $(CH_3)_2S$, respectively, and of the $[Pt(bipy-H)]^+$ fragment (**2**) resulting from the combined elimination, that is, $CH_4/(CH_3)_2S$.

Labeling experiments with $[Pt(bipy)(CH_3)((CD_3)_2S)]^+$ and $[Pt([D_8]bipy)(CH_3)((CH_3)_2S)]^+$ as precursor ions reveal that methane is generated from the (intact) Pt-bound methyl group together with a hydrogen atom which is provided mostly by the bipy ligand (ca. 65 %); only up to 35 % originate from the dimethylsulfide group. As to the evaporation of dimethylsulfide from **1**, this process is a clean reaction in that prior to ligand loss no hydrogen-exchange reactions of the ligands of **1** seem to occur in the gas phase. When mass selected [**1**−CH_4] is subjected to a collision experiment, the major reaction amounts to the elimination of Δ*m* 28. CID experiments with the labeled ions $[Pt(bipy-H)((CD_3)_2S)]^+$ and $Pt([D_8]bipy-D)((CH_3)_2S)]^+$ result in losses of Δ*m* 31 and 32 from the former compared to Δ*m* 28 and 29 from the latter precursor ion. While the relative ratios of Δ*m* 31 versus 32 and of Δ*m* 28 versus 29 vary with the collision energy applied, at $E_{lab} = 10$ eV the two channels are of comparable importance for each isotopologue. Obviously, in the course of this reaction *one* (and only one) hydrogen atom of the heterocyclic ligand is exchanged with a hydrogen atom of the dimethylsulfide group prior to the elimination of ethene. The occurrence of such a process is further supported by CID of the ion [**1**−CH_4−C_2H_4], in which one observes a signal due to the loss of Δ*m* 34 (H_2S) while in the spectrum of the respective ion generated from $[Pt(bipy)(CH_3)((CD_3)_2S)]^+$ this signal splits into Δ*m* 35 and 36 (in a 1:1 ratio).

As will be shown later, all these findings can consistently be explained by invoking a gas-phase "roll-over" cyclometalation of **1** in the course of its fragmentation; indirect support that the final product does indeed correspond to cyclometalated **2** is provided experimentally as well as by theory.

For example, DFT-based calculations reveal that the "roll-over" product **2** is 138 kJ mol^{-1} more stable than its conceivable isomer **3** (X = CH); the latter ion would arise upon an energetically demanding activation of the C(6)–H bond accompanied by a complete sacrifice of the stabilizing chelation of the platinum center by the nitrogen atom of the second pyridine ring.

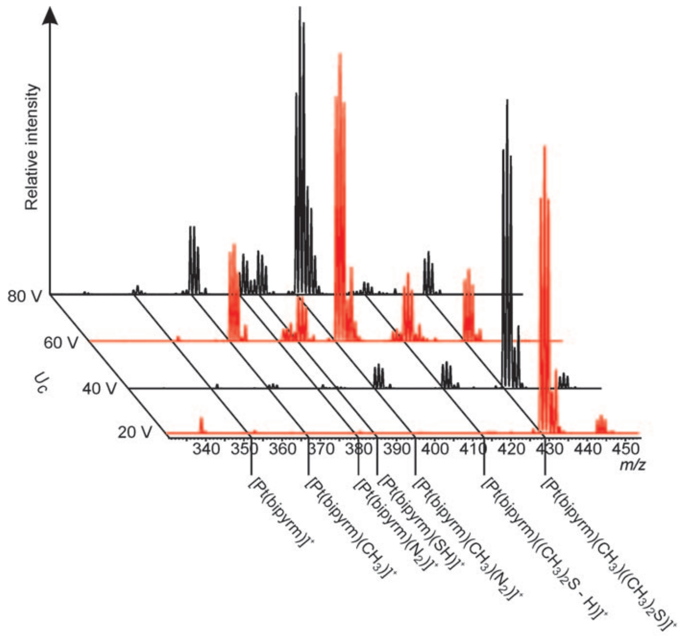

Figure 3. ESI source mass spectra of a dilute methanolic solution of [Pt$(CH_3)_2(\mu\text{-}(CH_3)_2S)]_2$ and 2,2′-bipyrimidine at different cone voltages.

Using 2,2′-bipyrimidine (bipyrm) instead of bipy as a ligand leads to the ion-source spectra shown in Figure 3. From [Pt(bipyrm)$(CH_3)((CH_3)_2S)]^+$ (**4**) a signal due to the loss of CH_4 is observed as well, but the fourth hydrogen atom is provided exclusively by the dimethylsulfide group as unequivocally shown by labeling experiments with the isotopologous $(CD_3)_2S$-containing complex of **4**, which shows no discernible contribution from the heterocyclic C–H bonds. Further, in the collision-induced formation of ethene from [Pt(bipyrm)$((CD_3)_2S{-}D)]^+$, no hydrogen/deuterium exchange precedes the reaction and exclusive elimination of C_2D_4 is observed. As the 2,2′-bipyrimidine complex **4** (Scheme 3) lacks a C(3)–H bond, a "roll-over" cyclometalation is impossible for this substrate on structural ground. Consequently, and as shown later in the context of the discussions of the ion/molecule reactions of [Pt(bipy–H)]$^+$ (**2**) with dimethylsulfide, the very existence of a structural unit such as **2** constitutes a prerequisite for the exchange of one hydrogen atom of the heterocycle with the hydrogen atoms of the dimethylsulfide ligand coordinated to the platinum core. In Table 1, CID data for [Pt(L)$(CH_3)((CH_3)_2S)]^+$ cations with L = 2-phenyl pyridine (phpy), 2,2′-bipyridine (bipy), 2,2′-pyridylpyrimidine (pypyrm), and 2,2′-bipyrimidine (bipyrm) is summarized. Fully consistent with the proposed "roll-over" mechanism, the loss of methane is most pronounced for phpy, which does not require a "roll-over" prior to activation of an aromatic C–H bond, and in the case of bipyrm the consecutive $CH_4/(CH_3)_2S$ loss is of no importance.

Table 1. Product branching ratios (normalized to Σ = 100) in the CID spectra of mass-selected [Pt(L)$(CH_3)((CH_3)_2S)]^+$ cations with L = 2-phenyl pyridine (phpy), 2,2′-bipyridine (bipy), 2,2′-pyridylpyrimidine (pypyrm), and 2,2′-bipyrimidine (bipyrm) at a collision energy of E_{lab} = 25 eV.

L	$-CH_4$	$-(CH_3)_2S$	$-(CH_4/(CH_3)_2S)$	LH^+
phpy	61	2	27	10
bipy	9	59	26	6
pypyrm	3	73	6	18
bipyrm	6	74	2	20

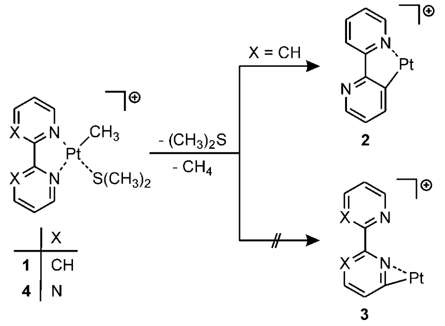

Scheme 3. Conceivable cyclometalation pathways for Pt^{II} complexes of 2,2′-bipyridine (X = CH) and 2,2′-bipyrimidine (X = N).

Next, the results of the DFT-based calculations for the process **1**→**2** are mentioned briefly with a focus on the energetics for the competitive eliminations of CH_4 and $(CH_3)_2S$. For the former, only the "roll-over" path will be dealt with, as activation of a pyridine C–H bond corresponds to the major channel (ca. 65 %) as compared to C–H-bond activation of the dimethylsulfide ligand. Also the details of the combined C_2H_4/H_2S loss from [**1**–CH_4] will not be addressed in the present context, as the mechanism(s) of this formal dehydrosulfurization[24] will be discussed in some detail further below; there, we will describe the ion/molecule reaction of **2** with $(CH_3)_2S$ leading to the loss of C_2H_4. Structural details and selected geometry data of the relevant species involved in the process **1**→**2** are collected below (selected bond lengths given in Å of the minima and transition structures depicted in Figure 4; charges have been omitted for the sake of clarity), and a simplified potential-energy surface (PES) is given in Figure 4. The brief discussion of the PES will be arranged along the color code used in Figure 4 for the various mechanistic alternatives.

In the overall endothermic transformation **1**→**2**, the four competing pathways for ligand evaporation accompanied with cyclometalation fall into two categories which are clearly distinguished energetically. In the most favored one, the first step corresponds to methane elimination in the pres-

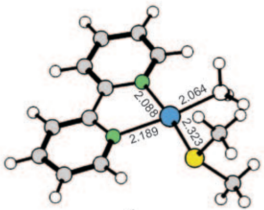

1

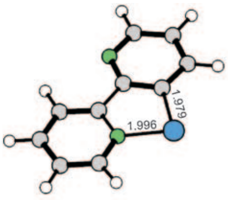

2

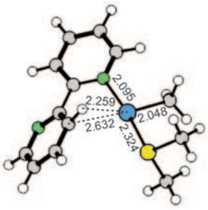

5

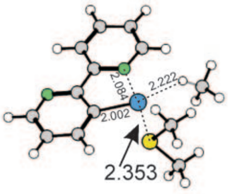

6

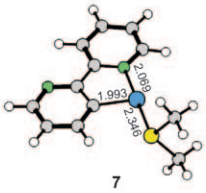

7

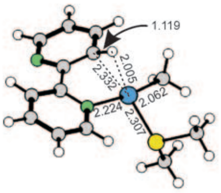

8

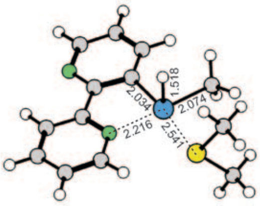

9

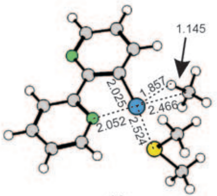

10

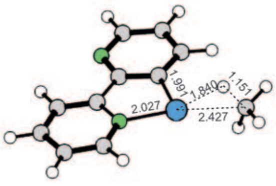

11

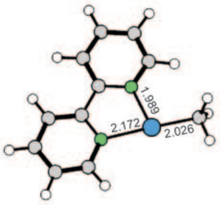

12

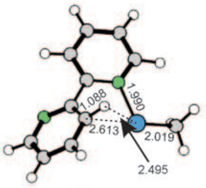

13

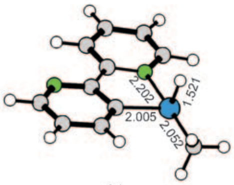

14

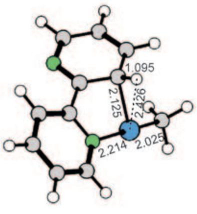

15

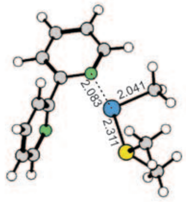

TS1/5

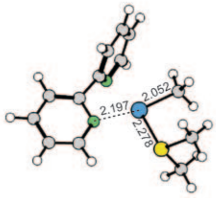

TS1/8

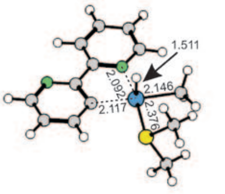

TS5/6

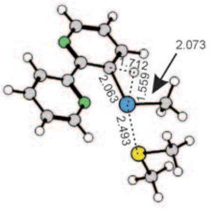

TS8/9

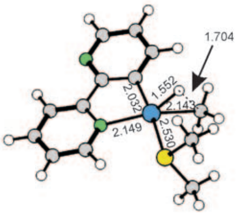

TS9/10

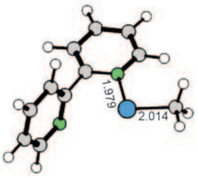

TS12/13

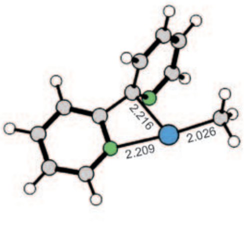

TS12/15

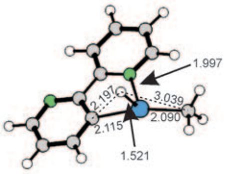

TS13/14

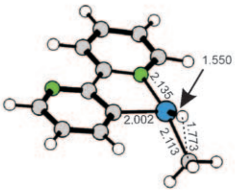

TS14/11

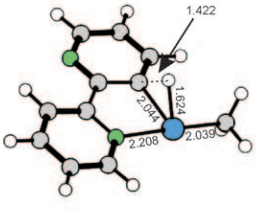

TS15/14

© 2008 Wiley-VCH Verlag GmbH & Co. KGaA, Weinheim

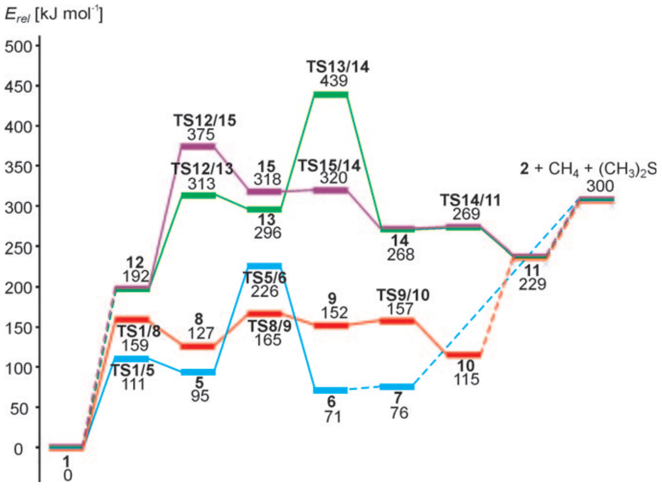

Figure 4. Schematic PES for the reaction: [Pt(bipy)(CH$_3$)((CH$_3$)$_2$S)]$^+$ (**1**)→[Pt(bipy−H)]$^+$ (**2**)+CH$_4$+(CH$_3$)$_2$S (see text for details).

ence of the stabilizing dimethylsulfide ligand (pathways given in blue and red); in contrast, when the (CH$_3$)$_2$S ligand is initially evaporated from **1** (i.e. **1**→**12**), the remaining bond activation and bond formation steps (indicated by the green and pink curves in Figure 4) are significantly higher in energy. In fact, according to the DFT data the energy requirements of several of the transition structures that connect intermediate **12** with the final products **2**/CH$_4$/(CH$_3$)$_2$S exceed the exit channel substantially. Thus, this pathway is unlikely to play a role in the formation of **2** near threshold conditions of the CID experiments, even though the routes via **2** might compete at elevated collision energies. In contrast, in the initial step for the production of CH$_4$, complexes **6** and **10** (either of which may then serve as intermediates for the final evaporations of CH$_4$ and (CH$_3$)$_2$S to generate **2**) are more easily accessible energetically and the rate-determining steps **5**→**6** and **8**→**9** are associated with the "rollover" metalation reaction, that is, the activation and transformation of an agostic C(3)−H bond. There are, however, subtle mechanistic differences, and a few of them are worthy of mentioning. In the "blue" reaction path, **1**→**5**→**6**→**7**→**2**, platinum retains its formal oxidation state Pt^{II}, and the crucial step **5**→**6** has the signature of a σ-bond metathesis reaction.[25] In contrast, the related steps **8**→**9**→**10** are better described in terms of an oxidative addition/reductive elimination reaction that is, Pt^{II}→Pt^{IV}→Pt^{II}. Another, rather general structural aspect concerns the geometric arrangement of the dimethylsulfide ligand in the (CH$_3$)$_2$S complexes. A preference for a *trans*-alignment of the N-Pt-S unit seems to exist, as shown for **6** and **7**.[26] This feature bears some resemblance with the X-ray structure of [Pt(Cl)(L−H)((CH$_3$)$_2$S)] with L=6-*tert*-butyl-2,2′-bipyridine;[6h] in this cyclometalated complex, the (CH$_3$)$_2$S ligand occupies a *trans*-position with a Pt−N-bond length of 2.042 Å and a Pt−S-bond length of 2.263 Å. The DFT-derived data for the corresponding N-Pt-S unit in the gas-phase, structure **7**, are 2.069 and 2.346 Å, respectively. A stereoisomer of **7**, with a *cis* N-Pt-S alignment, could not be located as a minimum in our rather extensive PES screening.

As mentioned above, CID of [**1**−CH$_4$] yields a signal due to the loss of C$_2$H$_4$. This observation prompted us to address the ion/molecule reaction of (CH$_3$)$_2$S with mass-selected [Pt(bipy−H)]$^+$ (**2**), where the latter has been generated from **1** at U_c=60 V. The dominant product ions of the IMR at E_{lab} nominally set to 0 V (Figure 5) correspond to the loss of C$_2$H$_4$ (55 % of all product ions formed) and the generation of protonated bipy (*m*/*z* 157) with 15 % of the branching ratio. Obviously, the first process corresponds to a formal dehydrosulfurization of (CH$_3$)$_2$S and an oxidative C−C coupling of the two methyl groups to liberate C$_2$H$_4$. In the production of *m*/*z* 157, one hydrogen atom and one proton are transferred from the incoming (CH$_3$)$_2$S ligand to the (bipy−H) fragment, yielding (bipy+H)$^+$. When this ion/molecule reaction is conducted with (CD$_3$)$_2$S, the spectrum shown in Figure 6 is obtained. Obviously, all relevant signals, that is, losses of, for example, ethene (Δ*m* 28) and thiofor-

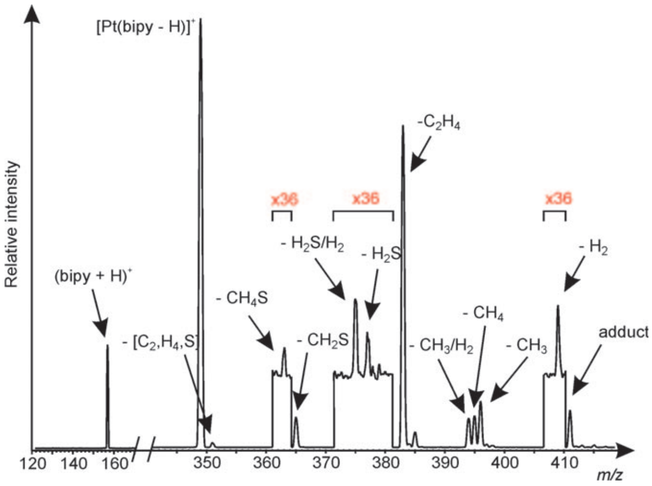

Figure 5. Ion/molecule reactions of mass-selected [Pt(bipy−H)]$^+$ (**2**) with (CH$_3$)$_2$S.

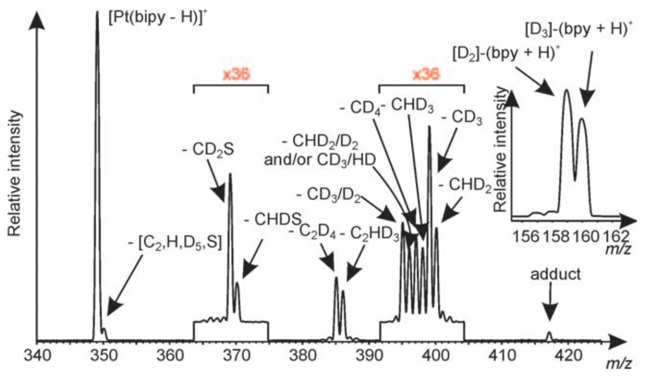

Figure 6. Ion/molecule reactions of mass-selected [Pt(bipy−H)]$^+$ (**2**) with (CD$_3$)$_2$S. The signals for the loss of protonated bipyridine are shown as inset.

© 2008 Wiley-VCH Verlag GmbH & Co. KGaA, Weinheim

maldehyde (Δ*m* 46) or the formation of protonated bipy, are split into doublets. For example, for the latter ion, one does not only observe a signal due to the expected transfer of only *two* deuterium atoms from the $(CD_3)_2S$ ligand to (bipy−H), resulting in *m*/*z* 159; rather, a third deuterium has been incorporated through hydrogen exchange giving rise to *m*/*z* 160. Similarly, in the eliminations of ethene and thioformaldehyde, the expected signals of C_2D_4 and CD_2S are accompanied by signals due to the eliminations of C_2D_3H and CDHS, respectively. Quite clearly, prior to these dissociation processes *one* (and only one) hydrogen atom from the heterocyclic (bipy−H) fragment undergoes an H/D exchange process with the dimethylsulfide ligand. Such a scenario is expected to occur for a cyclometalated structure **16** (Scheme 4) in which the still available C(3′)−H bond undergoes the H/D exchange with the dimethylsulfide ligand (depicted as RH in Scheme 4). Thus, an unprecedented reversible "roll-over" process is operative. For a system lacking this structural feature, as in the cyclometalated Pt^{II} complex **22** of 2′-pyridinyl-2-pyrimidine (pypyrm), one does not expect any of these exchange processes to occur. In fact, as shown in Figure 7, the ion/molecule reaction of mass-selected [Pt(pypyrm−H)]$^+$ with $(CH_3)_2S$ does not exhibit any evidence for H/D exchange between the two ligands prior to product formation.

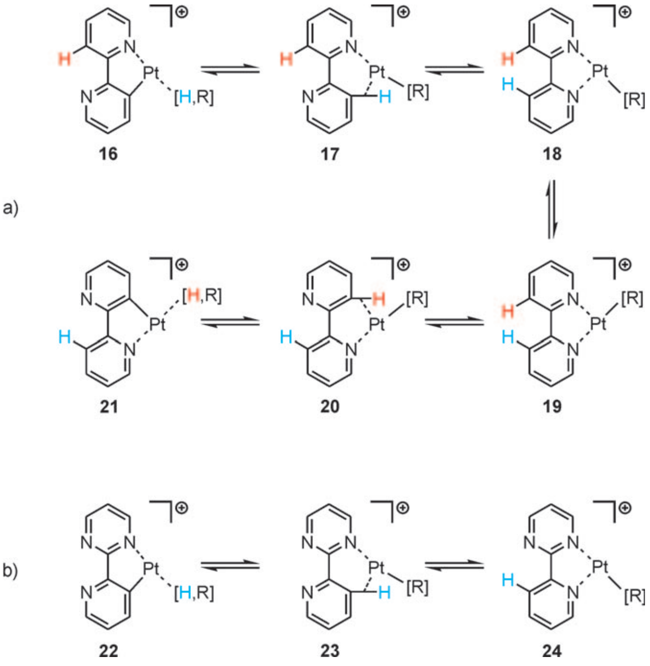

Scheme 4. a) Hydrogen exchange between C(3′)-H of a Pt-bound 2,2′-bipyridine fragment and RH (R stands for CH_3SCH_2); b) reversible hydrogen transfer from RH to a Pt-bound 2′-pyridinyl-2-pyrimidine fragment.

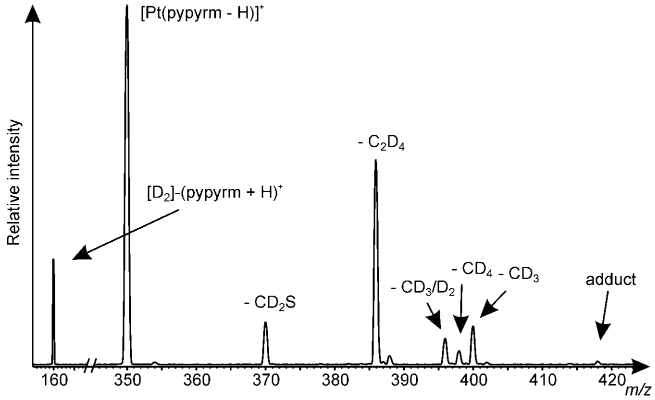

Figure 7. Ion/molecule reactions of mass-selected [Pt(pypyrm−H)]$^+$ with $(CD_3)_2S$.

A closer inspection of Figure 6 reveals, however, that the actual mechanism of ethene elimination, which forms the focus of our interest, actually seems more subtle than to follow a simple combination of intracomplex hydrogen exchange between ligands terminated by a specific transfer of "H_2S" from the dimethylsulfide ligand to the [Pt(bipy−H)]$^+$ core. Therefore, a rather extensive labeling study employing [D_8]bipy, CH_3SCD_3, and $(CD_3)_2S$, was conducted; the experimental isotope distributions in the formations of C_2H_{4-x} (x = 0–4) was subjected to a detailed kinetic modeling.[27] In this kinetic model, we take into account i) the existence of averaged primary kinetic isotope effects for the various transfers of H/D atoms (KIE_{trans}) and of a secondary isotope effect associated with the formation of $C_2H_{4-x}D_x$ (KIE_{sec}), ii) a statistical exchange process of *one* hydrogen/deuterium atom from the bipy fragment with any of the six hydrogen/deuterium atoms of the dimethylsulfide ligand (we abbreviate the fraction of this "scrambling" reaction f_{scr}), and iii) the possibility that the two hydrogen atoms of dimethylsulfide are transferred directly, that is, without H/D exchange, to the [Pt(bipy−H)]$^+$ fragment (f_{sel}). For the "direct" path we further distinguish two mechanistic variants, that is, a formal 1,1-transfer (both hydrogen atoms originate from the same methyl group) or a 1,3-process (the notations $f_{1,1}$ and $f_{1,3}$ are used for these two alternatives). As shown in Table 2, one

Table 2. Experimentally observed and computationally derived distributions for the formation of $C_2H_{4-x}D_x$ (x = 0–4) in the ion/molecule reactions of [Pt(bipy−H)]$^+$ (**2**) and [Pt([D_8]bipy−D)]$^+$ with dimethylsulfide (DMS) and its isotopologues.[a]

	[Pt(bipy−H)]$^+$			[Pt([D_8]bipy−D)]$^+$		
	DMS	[D_3]DMS	[D_6]DMS	DMS	[D_3]DMS	[D_6]DMS
C_2H_4	100 (100)	2.0 (2)	–	56.6 (57)	–	–
C_2H_3D	–	28.3 (28)	–	43.5 (43)	11.3 (11)	–
$C_2H_2D_2$	–	55.9 (56)	–		54.7 (54)	–
C_2HD_3	–	13.8 (14)	43.5 (44)		31.6 (32)	–
C_2D_4	–	–	56.6 (57)		2.4 (3)	100 (100)

[a] The distributions are normalized to Σ = 100%. Numbers given in parentheses refer to the experimental data.

obtains excellent agreement between the experimental findings for all six independent reactions and the kinetic modeling for the following modeling parameters: $f_{scr}=0.74$, $f_{sel}=0.26$, $f_{1,1}=0.32$, $f_{1,3}=0.68$; $KIE_{trans}=1.1$ and $KIE_{sec}=0.95$. As can be seen from these values, the loss of ethene is preceded by a rather strong but not complete scrambling ($f_{scr}=0.74$) of one hydrogen atom from the (bipy−H) ligand and the six hydrogen atoms from $(CH_3)_2S$. This is also reflected in the low value of 1.1 for KIE_{trans}. Moreover, for the selective channel one finds a preference for a 1,3-elimination mechanism ($f_{1,3}=0.68$).

Further insight into mechanistic aspects of the rather unusual C_2H_4 generation from the encounter complex $[Pt(bipy-H)]^+/(CH_3)_2S$ is obtained from DFT-based calculations. As applied for the reaction sequence **1**→**2**, also in the ion/molecule reaction of **2** with $(CH_3)_2S$ only singlet states are considered because the triplets are invariably much higher in energy. Further, here we report only the reaction path that commences with a C−H-bond activation of the incoming $(CH_3)_2S$ ligand, and we will confine ourselves to the 1,3-hydrogen-atom transfer variant which forms the major component in this rather complicated system (see Table 2). The conceivable initial activation of a C−S bond by oxidative insertion of platinum in this bond has also been addressed computationally.[27b] However, due to the unavoidable involvement of high-energy Pt^{VI} species in this path of bond activation and C−C-bond formation, this reaction variant was found to proceed via transition states that are located well above (> 115 kJ mol^{-1}) the entrance channel; thus, they do not play a role in the thermal experiment and will not be discussed here.

The simplified PES of the IMR of $[Pt(bipy-H)]^+$ with $(CH_3)_2S$ is shown in Figure 8, and relevant geometric details are shown below (selected bond lengths given in Å; charges omitted for clarity). The reaction commences with the formation of the rather stable encounter complex **7** (for the geometry of **7**, see above). The energy gained in this step is substantial (−224 kJ mol^{-1}) and is contained as ro-vibrational energy in the encounter complex to drive the system toward product formation. Actually, all intermediates and their connecting transition structures are located energetically below the entrance channel; the overall reaction to form C_2H_4 and $[Pt(bipy)(H)(S)]^+$ (**32**) is exothermic.[28] The most stable structure is **26** in which the C−H-bond activation of dimethylsulfide delivers a hydrogen atom for re-establishing the aromatic C−H bond of the nitrogen ligand, resulting in a formal coordination of deprotonated dimethylsulfide to the platinum center.[29,30] There are two steps which are rather high in energy. The first one, TS **7**/**25**, is associated with the platinum-mediated transfer of a hydrogen from the incoming $(CH_3)_2S$ ligand associated with Pt−C cleavage and C-H-bond formation (**7**→**25**); next, in a sequence of events **25** gives rise to **28** (from which also CH_2S may be liberated). The crucial C−C-bond forming-step, to generate a precursor for the eventual formation of C_2H_4, commences from **28** to give rise to **29**. The latter structure has all requirements to rearrange via a conventional γ-hydrogen transfer (**29**→**30**) followed by a cycloreversion of the metallacycle. This process (**30**→**31**), once more, is rather energy-demanding; in contrast, the evaporation of C_2H_4 from **31**, which terminates the dehydrosulfurization of $(CH_3)_2S$, is facile. While elimination of neutral ethene is also observed in the ion/molecule reaction of mass-selected $[Pt(pypyrm-H)]^+$ with $(CH_3)_2S$ (Figure 7), this does not hold true for the analogous reaction of $[Pt(phpy-H)]^+$ with $(CH_3)_2S$. Assuming a mechanism analogous to that depicted in Scheme 2 is operative for all three heterocyclic systems (Scheme 5), the deviating behavior of the $[Pt(phpy-H)]^+/(CH_3)_2S$ couple can be related to the step **25**→**26**, which is accompanied by an energy gain of about 105 kJ mol^{-1} for the bipy system because of the second nitrogen atom that coordinates to the platinum core in this step. In the related phpy system, however, no such coordination is possible; consequently, the exit channel would be higher by this amount of energy in comparison to the bipy system. In future work we will address various structural and mechanistic aspects of this technologically rather important process of hydrocarbon refining in more detail.

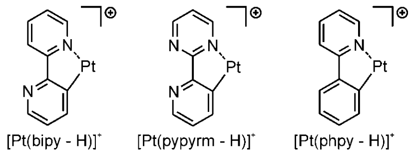

Scheme 5. Structural representations of $[Pt(bipy-H)]^+$ (**2**), $[Pt(pypyrm-H)]^+$, and $[Pt(phpy-H)]^+$.

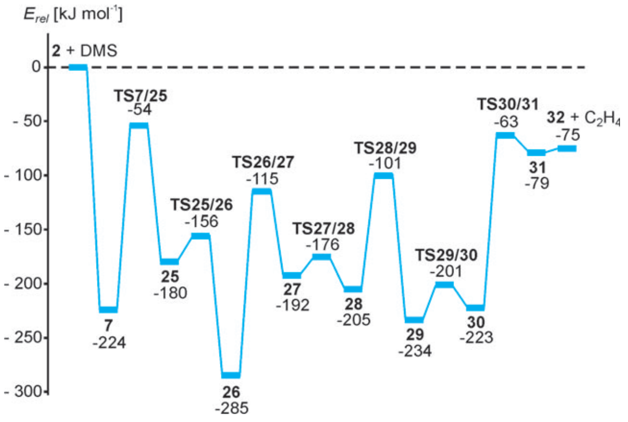

Figure 8. Simplified PES for the ion/molecule reaction of $[Pt(bipy-H)]^+$ (**2**) with $(CH_3)_2S$ to generate C_2H_4 (see text for details).

Conclusion

The combined experimental/theoretical investigation of the fragmentation behavior of cationic $[Pt(bipy)(CH_3)((CH_3)_2S)]^+$ (**1**) provides insight into various bond-activation and bond-coupling reactions promoted by cationic platinum

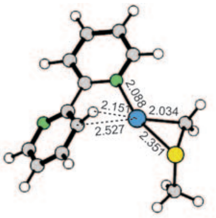

25

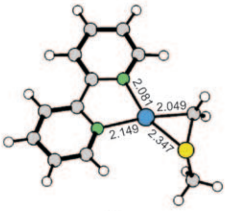

26

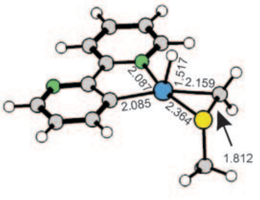

TS7/25

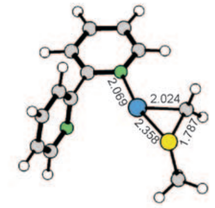

TS25/26

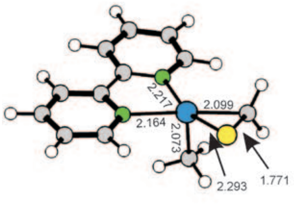

27

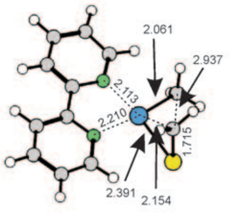

28

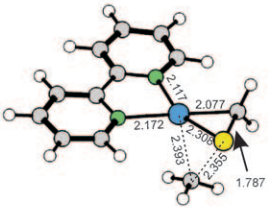

TS26/27

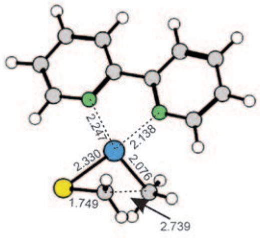

TS27/28

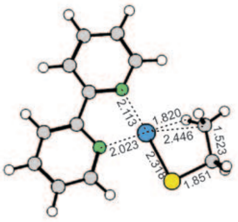

29

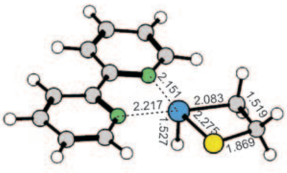

30

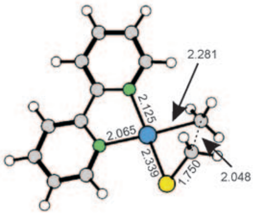

TS28/29

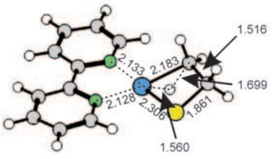

TS29/30

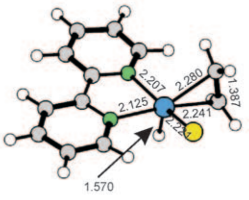

31

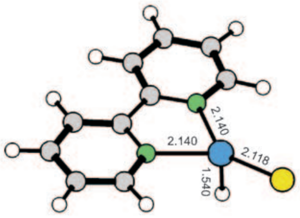

32

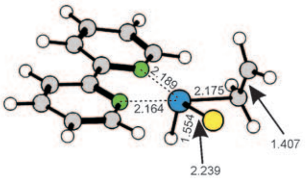

TS30/31

complexes in the gas phase. In the competitive loss of methane and dimethylsulfide, methane is mostly formed from the Pt-bound methyl group and one C(3)−H hydrogen atom from the bipy ligand, and a "roll-over" cyclometalation mechanism is operative. This reaction is without precedence in the gas phase. Further fragmentation yields the cyclometalated species [Pt(bipy−H)]$^+$ (**2**). The genesis of the latter ion was furthermore studied theoretically using DFT calculations. In ion/molecule reactions of [Pt(bipy−H)]$^+$ with dimethylsulfide we probe a part of the potential energy surface that is also accessed in the CID experiments of [**1**−CH_4]. Labeling experiments demonstrate that the expulsion of ethene is accompanied by an extensive scrambling of *one* (and only one) hydrogen atom from the heterocyclic ligand with the six hydrogen atoms of the dimethylsulfide unit. This, and other experiments, are best interpreted as evidence for the reversibility of the cyclometalation process in the gas phase. An extensive labeling study of this reaction permits to derive a kinetic model of the data, revealing a preferred 1,3-hydrogen transfer from dimethylsulfide to [Pt(bipy−H)]$^+$ in the course of ethene liberation. The ion/molecule reaction of [Pt(pypyrm−H)]$^+$ with dimethylsulfide further suggests that the "active" hydrogen in the bipy ligand must be the C(3)−H hydrogen atom and thus further support the operation of a reversible "roll-over" cyclometalation process. To elucidate the mechanism of the unusual oxidative C−C-coupling reaction in the transformation $CH_3SCH_3 \rightarrow CH_2{=}CH_2$, exploratory DFT calculations were carried out. As a main result, together with the experiment, the driving force for the whole reaction sequence is the formation of a second Pt–N coordination in the course of the retro "roll-over" process.

Acknowledgements

Financial support by the Fonds der Chemischen Industrie, the Academy of Sciences of the Czech Republic (Z40550506), and the Cluster of Excellence "Unifying Concepts in Catalysis", sponsored by the Deutsche Forschungsgemeinschaft and administered by the Technische Universität Berlin, is appreciated.

© 2008 Wiley-VCH Verlag GmbH & Co. KGaA, Weinheim

---

[1] *Comprehensive Supramolecular Chemistry* (Eds.: J. L. Atwood, J. E. D. Davide, D. D. MacNicol, F. Voegtle, J.-M. Lehn), Pergamon, Oxford, **1996**.

[2] P. Belser, S. Bernhard, E. Jandrasics, A. von Zelewsky, L. De Cola, V. Balzani, *Coord. Chem. Rev.* **1997**, *159*, 1–8.

[3] E. Drent, P. H. M. Budzelaar, *Chem. Rev.* **1996**, *96*, 663–682.

[4] A. Togni, L. M. Venanzi, *Angew. Chem.* **1994**, *106*, 517–547; *Angew. Chem. Int. Ed. Engl.* **1994**, *33*, 497–526.

[5] a) V. Katta, S. K. Chowdhury, B. T. Chait, *J. Am. Chem. Soc.* **1990**, *112*, 5348–5349; b) S. R. Wilson, A. Yasmin, Y. Wu, *J. Org. Chem.* **1992**, *57*, 6941–6945; c) C. L. Gatlin, F. Turec̀ek, T. Vaisar, *J. Am. Chem. Soc.* **1995**, *117*, 3637–3638; d) T. G. Spence, T. D. Burns, L. A. Posey, *J. Phys. Chem. A* **1997**, *101*, 139–144; e) T. G. Spence, T. D. Burns, G. B. Guckenberger, L. A. Posey, *J. Phys. Chem. A* **1997**, *101*, 1081–1092; f) T. G. Spence, B. T. Trotter, T. D. Burns, L. A. Posey, *J. Phys. Chem. A* **1998**, *102*, 6101–6106; g) J. Shen, J. Brodbelt, *J. Am. Soc. Mass Spectrom.* **1999**, *10*, 126–135; h) R. W. Vachet, J. H. Callahan, *J. Mass Spectrom.* **2000**, *35*, 311–320; i) J. Zhang, J. S. Brodbelt, *J. Mass Spectrom.* **2003**, *38*, 555–572; j) A. Harriman, R. Ziessel, J.-C. Moutet, E. Saint-Aman, *Phys. Chem. Chem. Phys.* **2003**, *5*, 1593–1598; k) R. E. Shepherd, J. M. Slocik, T. W. Stringfield, K. V. Somayajula, A. A. Amoscato, *Inorg. Chim. Acta* **2004**, *357*, 965–979; l) N. G. Tsierkezos, M. Diefenbach, J. Roithová, D. Schröder, H. Schwarz, *Inorg. Chem.* **2005**, *44*, 4969–4978.

[6] a) R. J. Watts, J. S. Harrington, J. Van Houten, *J. Am. Chem. Soc.* **1977**, *99*, 2179–2187; b) W. A. Wickramasinghe, P. H. Bird, N. Serpone, *J. Chem. Soc. Chem. Commun.* **1981**, 1284–1286; c) E. C. Constable, K. R. Seddon, *J. Chem. Soc. Chem. Commun.* **1982**, 34–36; d) S. Dholakia, R. D. Gillard, F. L. Wimmer, *Inorg. Chim. Acta* **1983**, *69*, 179–181; e) G. Nord, A. C. Hazell, R. G. Hazell, O. Farver, *Inorg. Chem.* **1983**, *22*, 3429–3434; f) P. J. Spellane, R. J. Watts, C. J. Curtis, *Inorg. Chem.* **1983**, *22*, 4060–4062; g) P. S. Braterman, G. A. Heath, A. J. MacKenzie, B. C. Noble, R. D. Peacock, L. J. Yellowlas, *Inorg. Chem.* **1984**, *23*, 3425–3426; h) G. Minghetti, A. Doppin, A. Zucca, S. Stoccoro, M. A. Cinellu, M. Manassero, M. Sanzour, *Chem. Heterocycl. Compd.* **1999**, *35*, 992–1000; i) A. Zucca, A. Droppin, M. A. Cinellu, S. Stoccoro, G. Minghetti, M. Manassero, *Organometallics* **2002**, *21*, 783–785; j) G. Minghetti, S. Stoccoro, M. A. Cinellu, B. Soro, A. Zucca, *Organometallics* **2003**, *22*, 4770–4777; k) A. Zucca, M. A. Cinellu, G. Minghetti, S. Stoccoro, M. Manassero, *Eur. J. Inorg. Chem.* **2004**, 4484–4490; l) S. Stoccoro, A. Zucca, G. L. Petretto, M. A. Cinellu, G. Minghetti, M. Manassero, *J. Organomet. Chem.* **2006**, *691*, 4135–4146; m) G. Minghetti, S. Stoccoro, M. A. Cinellu, G. L. Petretto, A. Zucca, *Organometallics* **2008**, *27*, 3415–3421.

[7] a) J. B. Fenn, *Angew. Chem.* **2003**, *115*, 3999–4024; *Angew. Chem. Int. Ed.* **2003**, *42*, 3871–3894; b) http://nobelprize.org./chemistry/laureates/2002/.

[8] For other, recent examples of gas-phase cyclometalation, see: a) C. Hinderling, D. A. Plattner, P. Chen, *Angew. Chem.* **1997**, *109*, 272–274; *Angew. Chem. Int. Ed. Engl.* **1997**, *36*, 243–244; b) C. Hinderling, D. Feichlinger, D. A. Plattner, P. Chen, *J. Am. Chem. Soc.* **1997**, *119*, 10793–10804; c) D. Schröder, H. Schwarz, N. Aliagada-Alcade, F. Neese, *Eur. J. Inorg. Chem.* **2007**, 816–821; d) M. Schlangen, J. Neugebauer, M. Reiher, D. Schröder, J. P. Lopez, M. Haryono, F. W. Heinemann, A. Grohmann, H. Schwarz, *J. Am. Chem. Soc.* **2008**, *130*, 4285–4294; e) B. Butschke, M. Schlangen, D. Schröder, H. Schwarz, *Helv. Chim. Acta* **2008**, *91*, 1902.

[9] a) D. Schröder, T. Weiske, H. Schwarz, *Int. J. Mass Spectrom.* **2002**, *219*, 729–738; b) C. Trage, D. Schröder, H. Schwarz, *Chem. Eur. J.* **2005**, *11*, 619–627.

[10] G. S. Hill, M. J. Irwin, C. J. Levy, L. M. Rendina, R. J. Puddephatt, *Inorg. Synth.* **1998**, *32*, 149–153.

[11] N. B. Cech, C. G. Enke, *Mass Spectrom. Rev.* **2001**, *20*, 362–387.

[12] http://winter.group.shef.ac.nk/chemputer/.

[13] D. Schröder, H. Schwarz, *Can. J. Chem.* **2005**, *83*, 1936–1940.

[14] a) D. Schröder, H. Schwarz, S. Schenk, E. Anders, *Angew. Chem.* **2003**, *115*, 5241–5244; *Angew. Chem. Int. Ed.* **2003**, *42*, 5087–5090; b) C. Trage, M. Diefenbach, D. Schröder, H. Schwarz, *Chem. Eur. J.* **2006**, *12*, 2454–2464; c) D. Schröder, M. Engeser, H. Schwarz, E. C. E. Rosenthal, J. Döbler, J. Sauer, *Inorg. Chem.* **2006**, *45*, 6235–6245; d) P. Gruene, C. Trage, D. Schröder, H. Schwarz, *Eur. J. Inorg. Chem.* **2006**, 4546–4552; e) B. Jagoda-Cwiklik, P. Jungwirth, L. Rulíšek, P. Milko, J. Roithová, J. Lemaire, P. Maitre, J. M. Ortega, D. Schröder, *ChemPhysChem* **2007**, *8*, 1629–1639.

[15] S. Feyel, D. Schröder, H. Schwarz, *J. Phys. Chem. A* **2006**, *110*, 2647–2654.

[16] a) C. Lee, W. Yang, R. G. Parr, *Phys. Rev. B* **1988**, *37*, 785–788; b) A. D. Becker, *J. Chem. Phys.* **1993**, *98*, 5648–5652.

[17] Gaussian 03, Revision C.02, M. J. Frisch, G. W. Trucks, H. B. Schlegel, G. E. Scuseria, M. A. Robb, J. R. Cheeseman, J. A. Montgomery, Jr., T. Vreven, K. N. Kudin, J. C. Burant, J. M. Millam, S. S. Iyengar, J. Tomasi, V. Barone, B. Mennucci, M. Cossi, G. Scalmani, N. Rega, G. A. Petersson, H. Nakatsuji, M. Hada, M. Ehara, K. Toyota, R. Fukuda, J. Hasegawa, M. Ishida, T. Nakajima, Y. Honda, O. Kitao, H. Nakai, M. Klene, X. Li, J. E. Knox, H. P. Hratchian, J. B. Cross, V. Bakken, C. Adamo, J. Jaramillo, R. Gomperts, R. E. Stratmann, O. Yazyev, A. J. Austin, R. Cammi, C. Pomelli, J. W. Ochterski, P. Y. Ayala, K. Morokuma, G. A. Voth, P. Salvador, J. J. Dannenberg, V. G. Zakrzewski, S. Dapprich, A. D. Daniels, M. C. Strain, O. Farkas, D. K. Malick, A. D. Rabuck, K. Raghavachari, J. B. Foresman, J. V. Ortiz, Q. Cui, A. G. Baboul, S. Clifford, J. Cioslowski, B. B. Stefanov, G. Liu, A. Liashenko, P. Piskorz, I. Komaromi, R. L. Martin, D. J. Fox, T. Keith, M. A. Al-Laham, C. Y. Peng, A. Nanayakkara, M. Challacombe, P. M. W. Gill, B. Johnson, W. Chen, M. W. Wong, C. Gonzalez, J. A. Pople, Gaussian, Inc., Wallingford CT, **2004**.

[18] A. Schafer, C. Hubers, R. Ahlrichs, *J. Chem. Phys.* **1994**, *100*, 5829–5835.

[19] The basis sets and ECPs correspond to the revision from June 27, **1997**, of the Stuttgart/Dresden groups. Also see: a) D. Andrae, U. Haeussermann, M. Dolg, H. Stoll, H. Preuss, *Theor. Chim. Acta* **1990**, *77*, 123–141; b) M. Dolg, H. Stoll, H. Preuss, R. M. Pitzer, *J. Phys. Chem.* **1993**, *97*, 5852–5859; c) K. A. Peterson, D. Figgen, M. Dolg, H. Stoll, *J. Chem. Phys.* **2007**, *126*, 124101.

[20] a) K. Fukui, *J. Phys. Chem.* **1970**, *74*, 4161–4163; b) K. Fukui, *Acc. Chem. Res.* **1981**, *14*, 363–368; c) C. Gonzalez, H. B. Schlegel, *J. Phys. Chem.* **1990**, *94*, 5523–5527.

[21] N. Tsierkezos, D. Schröder, H. Schwarz, *J. Phys. Chem. A* **2003**, *107*, 9575–9581.

[22] While the present experiments do not allow to assign a specific structure to $[\mathbf{1}{-}CH_4{-}C_2H_4]$, DFT calculations predict the Pt^{II} compound $[(bipy)Pt(SH)]^+$ as the most stable isomer compared to $[Pt(bipy{-}H)(SH_2)]^+$ (64 $kJ\,mol^{-1}$ higher in energy) and the formal Pt(IV) species $[Pt(bipy)(S)(H)]^+$ (111 $kJ\,mol^{-1}$ higher in energy).

[23] For further details of the appearance energy measurements, see: reference [14].

[24] We note, that dehydrosulfurization (DHS) is formally related to the industrially extremely important hydrodesulfurization (HDS) reaction of organic sulfur compounds: a) D. Stirling, *The Sulfur Problem: Cleaning up Industrial Feedstocks, RSC Clean Technology Monographs*, Royal Society of Chemistry, Cambridge, **2000**; b) R. A. Sánchez-Delgado, *Organometallic Modeling of the Hydrodesulfurization and Hydrodenitrogenation Reactions*, Kluwer Academic, Boston, **2002**; c) E. Furimsky, *Catal. Rev. Sci. Eng.* **2005**, *47*, 297–489; d) J. Ancheyta, M. S. Rana, E. Furinsky, *Catal. Today* **2005**, *109*, 1–2; e) For other gas-phase variants of dehydrosulfurization, see: K. Eller, S. Akkök, H. Schwarz, *Helv. Chim. Acta* **1990**, *73*, 229–238 and K. Eller, S. Akkök, H. Schwarz, *Helv. Chim. Acta* **1991**, *74*, 1609–1621; f) B. Butschke, M. Schlangen, D. Schröder, H. Schwarz, *Int. J. Mass Spectrom.*, in press.

[25] For recent, systematic experimental/computational studies of mechanistic variants of gas-phase, metal-mediated C−H bond activation, see: a) M. Armélin, M. Schlangen, H. Schwarz, *Chem. Eur. J.* **2008**, *14*, 5229–5236; b) M. Schlangen, H. Schwarz, *Helv. Chim. Acta*, in press.

© 2008 Wiley-VCH Verlag GmbH & Co. KGaA, Weinheim

[26] For a review of the *trans*-effect, see: F. R. Hartley, *Chem. Soc. Rev.* **1973**, *2*, 163–179.

[27] For details, see: a) B. Butschke, M. Schlangen, D. Schröder, H. Schwarz, *Z. Naturforsch. B* **2007**, *62b*, 309–313; b) B. Butschke, Diploma Thesis, Technische Universität Berlin, **2008**.

[28] Although $[Pt(bipy)(S)(H)]^+$ is not the most stable isomer,[22] the calculated reaction pathway can explain the experimental result of ethene liberation in the reaction of **2** with dimethylsulfide. An isomerisation process $[Pt(bipy)(S)(H)]^+ \rightarrow [Pt(bipy)(SH)]^+$ was therefore not further investigated.

[29] For experimental as well as theoretical studies about the fragmentation of $CH_3SCH_2^{+/0}$ see: a) B. van de Graaf, F. W. McLafferty, *J. Am. Chem. Soc.* **1977**, *99*, 6806–6810; b) W. J. Broer, W. D. Weringa, W. C. Nieuwpoort, *Org. Mass Spectrom.* **1979**, *14*, 543–549; c) D. W. Kuhns, T. B. Tran, S. A. Shaffer, F. Tureček, *J. Phys. Chem.* **1994**, *98*, 4845–4853; d) S.-W. Chiu, Y.-S. Cheung, N. L. Ma, W.-K. Li, C. Y. Ng, *J. Mol. Struct.* **1998**, *452*, 97–115; e) S.-W. Chiu, Y.-S. Cheung, N. L. Ma, W.-K. Li, C. Y. Ng, *J. Mol. Struct.* **1999**, *468*, 21–37; f) S.-W. Chiu, K.-C. Lau, W.-K. Li, N. L. Ma, Y.-S. Cheung, C. Y. Ng, *J. Mol. Struct.* **1999**, *490*, 109–124; g) Y.-J. Chen, P. T. Fenn, K.-C. Lau, C. Y. Ng, C.-K. Law, W.-K. Li, *J. Phys. Chem. A* **2002**, *106*, 9729–9736.

[30] Also interesting in this context are the following references about the dissociation and thermolysis of dimethylsulfide: a) L. G. S. Shum, S. W. Benson, *Int. J. Chem. Kinet.* **1985**, *17*, 749–761; b) H. Nagai, H. Ohmura, F. Ito, T. Nakanaga, M. Tachiya, *J. Chem. Phys.* **2006**, *124*, 034304.

Received: August 11, 2008
Published online: November 10, 2008